Case Studies on Cosmic Noise Absorption At Maitri During Thirtieth Indian Scientific Expedition to Antarctica

Jayanta K. Behera [1*], Ashwini K. Sinha [1], Ajay Dhar [1], Sachin Labde [1] and K. Jeeva [3]

1 Indian Institute of Geomagnetism, New Panvel (W), Navi Mumbai 410 218, India.
2 National Centre for Polar and Ocean Research, Headland Sada, Vasco-da-Gama, Goa 403 804, India.
[3] Equatorial Geophysical Research Laboratory, VittalapuramVilakku, Krishnapuram, Maharajanagar, Tirunelveli 627 011, India.

Abstract

Cosmic noise absorption (CAN) at high latitudes is a typical manifestation of enhanced precipitation of energetic charged particles during a magnetospheric substorm. Present analysis demonstrates the energetic particles precipitate to the high latitude ionosphere during subtorms, affecting upper and lower regions of the ionosphere simultaneously. Previous studies have reported that intense and short-lived CNA events associated with substorms are mostly observed in the midnight sector of the auroral oval. In the current study, we have examined such type of CNA events predominantly occurring during 0000-0600 UT (2300-0500 MLT) at an Indian Antarctic station Maitri (corrected geomagnetic (CGM) coordinates 62.59^0 S, 53.59^0 E), which is located at the equatorward edge of the auroral oval. Absorption events related to isolated substorm and storm-time substorms exhibit distinct features in terms of their intensity and extent in latitude and longitude. Our study suggests that the maximum intensity of CNAs depends on the interplanetary conditions, such as, the solar wind speed, southward component of IMF *Bz*, and duskward component of IEF *Ey*. Moreover, the role of duskward component of IEF E*y* is more noteworthy than other interplanetary parameters.

Keywords: *Cosmic noise absorption, Imaging Riometer, Substorm, Geomangetic storm*

1. Introduction

The disturbance created in the auroral ionosphere by precipitation of energetic particles during different processes has been of immense interest for the polar researchers (e.g., Newell and Meng, 1992; Burns et al. 1990; Meredith et al.,

---

* Corresponding Author- Present Address- Pillai HOC College of Arts and Science and Commerce, Rasayani

2011; Wing et al., 2013, etc.]. Magnetospheric substorms are known to populate nightside inner magnetosphere and auroral ionosphere with electrons and ions of wide energy ranges [Birn et al, 1997; Wing et al., 2013]. Effects of enhanced population of energetic particles have been extensively studied using ground and satellite based observations [e.g., Arnoldy, 1974; Sotirelis et al., 2013 and references therein].

The energies of softer electrons (energy < 10 keV) precipitating to the auroral ionosphere are absorbed in the E and F regions of the ionosphere and create magnificent optical auroral emissions. Additionally, low energy electrons enhance the auroral currents (electrojets) that can be easily monitored through magnetometers. Electrons of harder energies (> 20 keV) reach to the D region of the auroral ionosphere [Wilson and Stoker, 2002; Baker et al., 1982; Meredith et al., 2011]. Transient changes of harder electron densities in the lower ionosphere could additionally be monitored by Riometer (***R***elative ***I***onospheric ***O***pacity ***meter***). Incoming intergalactic cosmic radio waves to the Earth are absorbed to different degrees while passing through the ionosphere depending upon electron densities [Hargreaves, 1969]. Thus, cosmic noise absorption (CNA) provides an indirect method for diagnostics of the state of the ionosphere. Moreover, the total energy budget entered into the magnetosphere can be simultaneously monitored by PC-index and CNA, as it has been observed that CNA is unanimously dependent upon the geomagnetic activity level, which is characterized by PC-index [Alexander Frank-Kamenetesky and Oleg Troshichev, 2011].Various types of CNAs are commonly observed, e.g., F-region absorption, sudden cosmic noise absorption (SCNA), polar cap absorption (PCA), Auroral Substorm Absorption (ASA), dayside absorption spike events, poleward progressing absorption (PPA), etc., it is often possible to distinguish different types of absorption events on the basis of their appearances in the recordings of absorption intensities combined with knowledge of latitude, local time and season during the observations [Stauning, 1996].

Magnetospheric substorms initiate near midnight [Akasofu, 1968; Singh et al., 2012], as a result of which associated CNA events are often observed in the midnight sector of the auroral region during different phases of auroral substorms [Hargreaves, 1974; Jussila et al., 2004]. Generally, night-time CNA events are produced due to the precipitation of energetic electrons along the field lines from the injection region. However occasionally substorm associated CNA events are observed towards morning or even noon sectors due to eastward drift of electrons [Kavanagh et al., 2002; Birch et al., 2013].

Numerous studies on the substorm-associated CNAs have been carried out in the past using wide as well as narrow beam riometers [Ranta et al., 1981; Nielsen, 1980; Kikuchi et al., 1990]. With further advancement in instrumentation, multi-narrow-beam imaging riometers [Detrick and

Rosenberg, 1990; Browne et al., 1995] were utilized to study the dynamics of substorms and CNA signatures on a relatively smaller spatial scale [Kavanagh, 2002; Kellerman and Makarevich, 2011; Hargreaves et al., 1997].

It has been reported that CNAs exhibit distinct features during different phases of a substorm, e.g., reduction in CNA during the growth phase due to the stretching of field lines and enhancement preceding substorm onset by a few minutes due to the dipolarization [Kellerman and Makarevich, 2011]. Dispersionless plasma injections into the inner magnetosphere are typical feature of a substorm onset [e.g., Birn et al, 1997]. CNA observed by a suitably located riometer has been demonstrated to be an effective tool for ground-based identification of dispersionless electron injections [Spanswick et al., 2007].

Electromagnetic and plasma properties in the near-Earth environment are closely related to changes in the solar wind parameters, e.g., southward orientation of the interplanetary magnetic field (IMF *Bz*) drive storms and substorms [Kullen and Karlsson, 2004; Gonzalez and Tsurutani, 1987], high speed solar wind streams generate HILDCAA events [Tsurutani and Gonzalez, 1987], pressure pulse compresses the magnetosphere and induce auroras [Liou et al., 2007], etc. CNA variations in response to the changes in the interplanetary conditions have been extensively examined [Meredith, et al., 2011; Korotova et al., 1997; Behera et al., 2014].

In this study, we have examined substorm-associated CNA absorptions observed at an Indian Antarctic station – Maitri (MLAT ~ 62° S) in relation to the interplanetary conditions. Our station being located towards the equatorward boundary of the auroral oval [Hanchinal et al, 1996], occurrences of substorm associated typical signatures of magnetic variations and CNAs are relatively less frequent in comparison to those identified by AL negative bays.

2. Data set and event selection

A 38.2 MHz (4 x 4 system) was installed at Indian Antarctic station, Maitri (Geographic coordinates: 70.75°S, 11.73°E; CGM coordinates: 62.59°S, 53.59°E; L=5; MLT ≈ UT – 1) during the austral summer 2009-2010. Further details on the riometer system can be found in Behera et al. [2014]. In the present study, riometer and digital fluxgate magnetometer (DFM) data from Maitri have been used for the period November 2010 to October 2011 when both instruments were simultaneously operational. Location of Maitri is such that it comes under the influence of Sq currents during geomagnetic quiet conditions [Vichare et al., 2012] whereas during disturbed conditions auroral electrojets determine geomagnetic field variations at Maitri [Arun et al., 2005].

For identification of substorm events, we used the conventional AL index available from the webpage of WDC, Kyoto (http://wdc.kugi.kyoto-u.ac.jp/aeasy/index.html). During the local night time at Maitri (2300-0500 MLT), AL, H-component variations at Maitri (MAI-H) and absorption data were visually scanned over the selected interval for selection of events. Maitri being in the southern hemisphere (in opposite hemisphere of AL stations) and near equatorward boundary of the auroral oval, AL negative bays are not always evident or comparable with MAI-H. Only those events were considered as substorm absorptions events for which sharp AL negative bay attained values < -150 nT followed by concurrent westward electrojet signature (MAI-H < - 70 nT) over Maitri and CNA > 0.2 dB. We ignored cases when there were significant (more than 15 minutes) delays between the onsets of MAI-H depression and CNA absorption.

We identified 31 clear substorm absorption events at Maitri over the selected one year duration. Fig. 1 shows distribution of events during magnetic local night hours. Events are mostly confined to pre-midnight and early dawn hours and this may be attributed to substorms primarily occurring around magnetic mid-night hours and the location of Maitri. We additionally examined SYM-H index during the selected events. It was observed that 26 absorption events occurred during moderate to weak storms (SYM-H < -30 nT), whereas only 5 events were not related to storm (SYM-H > -30 nT).

In order to examine the selected events in relation to interplanetary conditions, we used IMF and solar wind data obtained from OMNIWeb (http://omniweb.gsfc.nasa.gov/form/omni_min.html),. OMNIWeb data are time shifted to the bowshock nose considering the travel time of solar wind from the location of observation [e.g., Weimer and King, 2008].

For the selected events, correlations among the intensities of the global AL index, MAI-H and CNA over Maitri have been shown in Fig. 2. Magnitudes of maximum depressions in the AL index (Max |AL|) and MAI-H (Max |H|), and corresponding maximum enhancement in CNA (Max (CNA)) were estimated for each event. The scatter plots for Max |AL| vs Max |H| (correlation coefficient, *r* = 0.86), Max |H| vs Max (CNA) (*r* = 0.79) and Max |AL| vs Max (CNA) (*r* = 0.67) have been shown in Fig. 2. This ensures that the selected absorption events are associated with substorms.

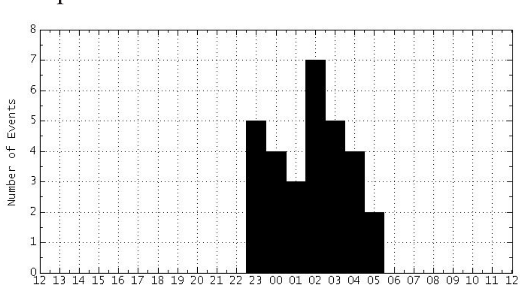

Fig. 1: *MLT distribution of onset of westward electrojet and CNA events for selected events at Maitri, Antarctica. Occurrence peaks around pre-midnight and early dawn hours.*

Linear relationship between the Max |AL| and Max |H| clearly suggests that during the selected events the maximum intensity of the westward auroral electrojet observed over Maitri during night time varies with substorms intensity observed by the global AL index in the northern hemisphere (Fig. 2a). For the selected events, intensity of CNA at Maitri also changes with varying intensities of the substorms or westward electrojet intensification at Maitri as shown in Figs. 2b and 2c. However, intensity of the absorption is better correlated with MAI-H intensity, which is obvious as both the observations are from the same location. Here, note that we have selected those absorption events which are accompanied by substorms; our figure 2c further demonstrates that being associated with substorms, how CNA varies with AL,

In the following section, we investigate CNA events observed at Maitri in relation to interplanetary conditions.

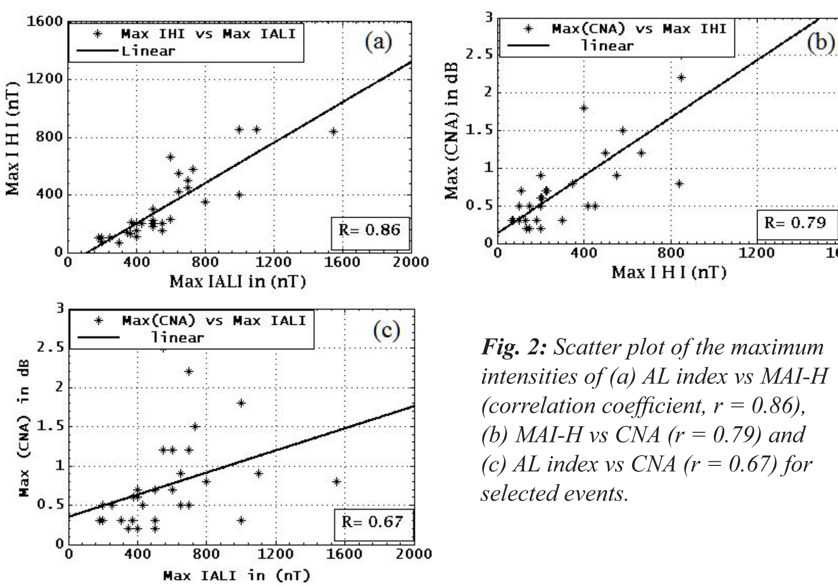

Fig. 2: *Scatter plot of the maximum intensities of (a) AL index vs MAI-H (correlation coefficient, r = 0.86), (b) MAI-H vs CNA (r = 0.79) and (c) AL index vs CNA (r = 0.67) for selected events.*

1. Observations

In this section firstly we present two typical CNA events associated with isolated substorms and one typical event associated with storm-time substorm to bring out the characteristic differences beween these two types of CNA events. The description of these events is followed by a subsection dealing with the effect of interplanetary conditions on CNA considering all the 31 events of one year selected as per the criteria mentioned in section 2.

3.1 Case studies

3.1.1 Event of 20 April 2011

A clear absorption event at Maitri was observed in association with an isolated substorm during 0300 – 0600 UT (0200 – 0500 MLT for Maitri). IMF *Bz* and *Vsw* taken from OMNIWeb is shown in the top two panels of Fig. 3. Occurrence of the substorm and its clear signatures in magnetometer and riometer data are evident as shown in the lower panels. Onset of sudden drop in AL leading to a negative bay started around 0410 UT, which appears to coincide with southward turning of IMF *Bz*. *Vsw* was steady (~ 450 km/s) during the event. It may be noted that the AL negative bay lasts longer than the MAI-H depression or CNA enhancement. Moreover, Max |AL| (700 nT) is higher than Max |H| (400 nT) for the event that could either be due to difference in the location of Maitri with respect to substorm onset region or due to the hemispherical asymmetry. Intensity of CNA maximized to about 1.0 dB during the substorm. SYM-H pattern (> -35 nT) suggests that the substorm event occurred during a weak storm.

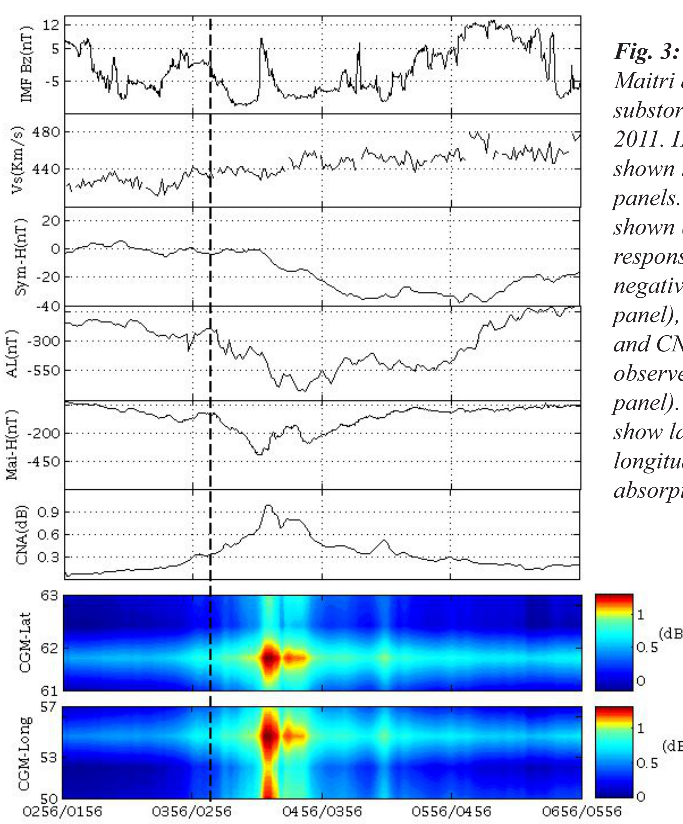

Fig. 3: *CNA event at Maitri during an isolated substorm on 20 April 2011. IMF Bz and Vsw are shown in the top two panels. Next, SYM-H is shown (third panel). In response to the AL negative bay (fourth panel), westward electrojet and CNA were clearly observed (fifth and sixth panel). Last two panels show latitude and longitude extent of the absorption.*

The last two panels in Fig. 3 represent latitudinal and longitudinal extent of the absorption for the event of 20 April 2011. Riometer observations show that absorption which in turn indicates particle precipitation maximizes around 62^0 CGM latitude and the longitudinal extent was over the complete field of view of the Maitri riometer. However the maximum CNA was observed around 55^0 CGM Longitude.

3.1.2 Event of 9 August 2011

A substorm leading to westward electrojet and CNA absorption signatures at Maitri started around 0450 UT. IMF *Bz* and *Vsw* for the event have been shown in the top two panels of Fig. 4. Substorm appears to have initiated with reduction in IMF *Bz*, whereas *Vsw* remained steady. The max |AL| was ~ 600 nT for the event. Maitri was located in dawn hours during the substorm. It can be seen that the westward auroral electrojet extended to Maitri about an hour later from the onset of substorm. Variation in CNA clearly follows MAI-H variation. During the substorm event SYM-H dropped up to -25 nT, thereby suggesting that the event occurred during a very weak storm.

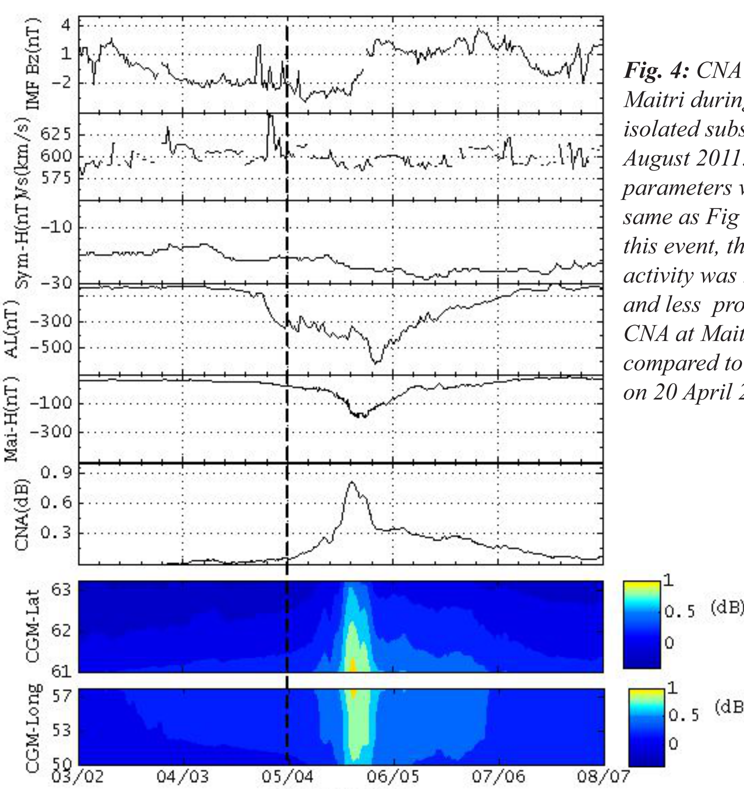

Fig. 4: *CNA event at Maitri during another isolated substorm on 9 August 2011. The parameters were plotted same as Fig 3. During this event, the substorm activity was moderate and less production of CNA at Maitri compared to the event on 20 April 2011.*

As shown in the bottom two panels for Fig. 4, precipitation of energetic electrons leading to CNA was mainly localized equatorward of Maitri station. Moreover, CNA was more intense in east longitudes during the event.

3.1.3 Event of 29 May 2011

A very intense storm-time substorm was initiated around 0500 UT, i.e., 0400 MLT for Maitri. The Dst index was ~ -66 nT for the event. AL negative bay started when IMF *Bz* was southward and *Vsw* was quite high (~650 km/s) for the event (Fig. 5). In a way similar to events discussed above, MAI-H or CNA variations lasted for shorter interval in comparison to AL variation. For this intense substorm event (Max |AL| ~ 1000 nT), Max |H| reached to about 800 nT and Max (CNA) exceeded 2 dB at Maitri. Unlike the above two events, SYM-H value relatively reduced more and has gone down to -64 nT during this event.

Several bursts of absorption covering almost the field of view of Maitri imaging riometer system were observed during the substorm as shown in the bottom two panels of Fig. 5.

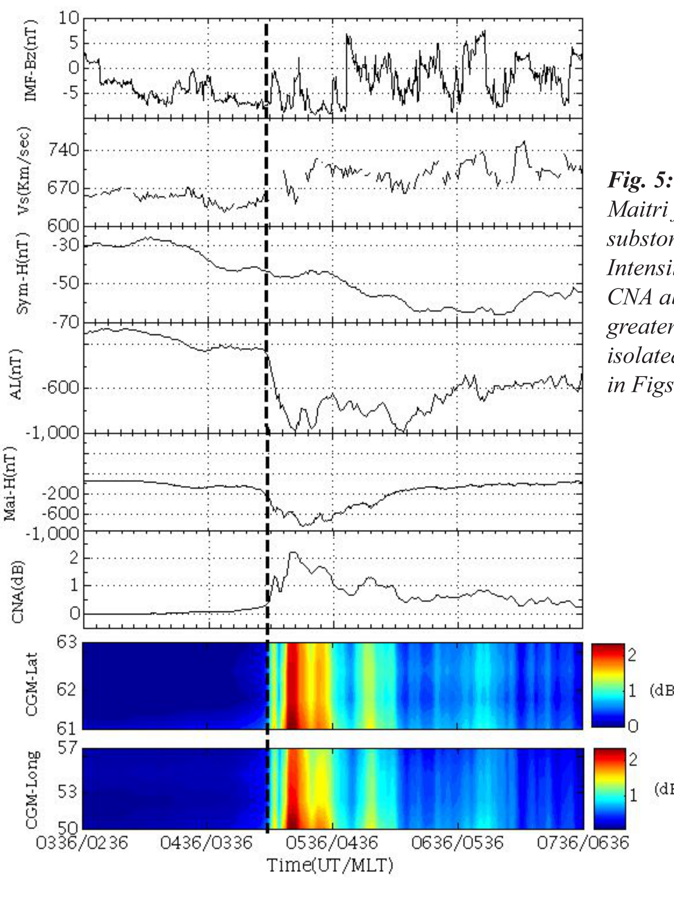

Fig. 5: *CNA event at Maitri for a storm-time substorm on 29 May 2011. Intensity and region of CNA absorption are far greater than those for isolated substorms shown in Figs. 3 and 4*

3.2 Effect of interplanetary conditions on CNAs

Geomagnetic activity is mainly controlled by the southward IMF *Bz*, *Vsw* and dawn-dusk interplanetary electric field, *Ey* (= - *Vsw* x *Bz*). In this section we examine variations of Max |AL|, Max |H| and Max (CNA) for all the selected events in relation to *Bz*, *Vsw* and *Ey*.

In a way similar to the maximum values of |AL|, |MAI-H| and CNA for each event, we calculated the highest magnitudes of southward IMF *Bz* (Max |IMF *Bz*), duskward IMF *Ey* (Max *Ey*) and *Vsw* (Max *Vsw*).

Scatter plots of Max |*Vsw*| vs Max (CNA) (*r* = 0.50), Max |*Bz*| vs Max (CNA) (*r* = 0.75) and Max *Ey* vs Max (CNA) (*r* = 0.85) are shown in Fig. 6. Poor correlation between the maximum *Vsw* and CNA intensity at Maitri suggests that solar wind speed alone does not effectively determine the level of particles precipitation over Maitri (Fig. 6a). However, for higher magnitude of southward IMF Bz during the substorm, precipitation of electrons leading to increased CNA (Fig 6b). Intensity of the absorption is highly correlated with the maximum duskward IMF *Ey* (Fig. 6c). It clearly suggests that the duskward oriented interplanetary electric field was the most important controlling factor for CNAs observed at Maitri.

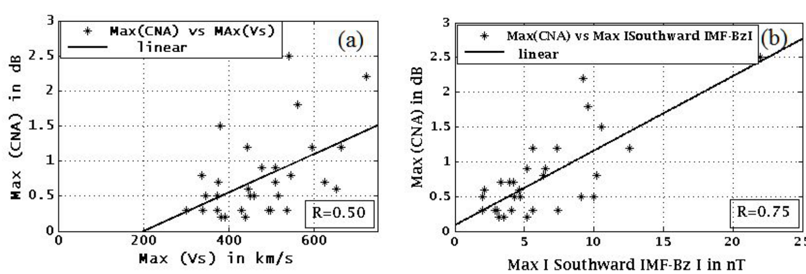

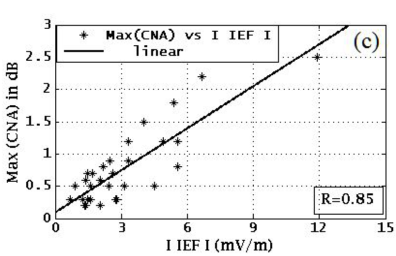

***Fig. 6:** Scatter plot of the maximum intensities of (a) Vsw vs CNA (correlation coefficient, r = 0.5), (b) southward IMF Bz vs CNA (r = 0.75) and (c) duskward IEF Ey vs CNA (r = 0.85) for selected events. CNA intensity at Maitri has strong dependence on IEF Ey.*

Moreover, for all the selected events IMF *Bz* was southward in the vicinity of onset of AL negative bay. The Max |IMF *Bz*| varied between 2 to 22 nT. Although substorm-associated CNA events occurred during a wide range of southward IMF Bz conditions, figure (6b) clearly shows most of the events were observed when IMF Bz was weakly southward. For the selected events, the Max |*Vsw*| varied from about 300 to 725 km/s (Fig. 6a). It is observed that the occurrence of absorption events at Maitri, however, do not have strong dependence on the solar wind speed.

4. Results and discussion

Precipitation of energetic electrons into the auroral ionosphere usually affect different regions depending upon their energies, e.g., westward auroral electrojet is driven by low energy electrons precipitated in the E-region, whereas higher energy electrons lead to cosmic radio noise absorption in the D-region [Wilson and Stoker, 2002; Baker et al., 1982]. During magnetospheric substorms (as identified by the AL index), we selected 31 associated events at Maitri based on concurrent response in the magnetometer and riometer data. Substorm-associated CNA events were mainly localized near local midnight, which is consistent with earlier observations [e.g., Kellerman and Makarevich, 2011].

The maximum intensities of MAI-H and CNA at Maitri were well correlated with the intensity of AL index (Fig. 2). However, we observed that the MAI-H negative bays were short-lived and corresponding maximum intensities (max |H|) were consistently lower than those for AL negative bays as shown in Figs. 3-5. AL index being the lower envelop of H component disturbance from about 10-12 stations [Davis and Sugiura, 1966], negative bay could last longer due to contributions from other stations where westward electrojet maximizes. Moreover, hemispherical asymmetry in the substorm signatures [Weygand and Zesta, 2008; Singh et al., 2012] and the location of Maitri station (equatorward of auroral oval in the southern hemisphere) could be other reasons for the difference between AL and MAI-H signatures.

High correlations of Max |H| vs Max (CNA) (Fig. 2b), and MAI-H vs CNA for individual substorm events (see Figs. 3-5) clearly suggest that softer and harder energy electrons, respectively affecting upper and lower regions of the ionosphere, simultaneously precipitate to the auroral ionosphere during sustorms.

Isolated and storm-time substorms mainly differ by the magnitude and extent [Feldstein et al., 2006; Partamies et al., 2013]. It is evident from Figs. 3 and 4 that for isolated substorm events, absorptions over Maitri were quite localized in latitude (< 2 degrees), but fairly wide in longitude (about 5 degrees). For storm-time substorm absorption was much intense and covers the entire field of view of the riometer (Fig. 5).

At Maitri station, most of the substorm-associated CNA events (26 out of 31) were observed during moderate to weak magnetic storms and predominantly under southward IMF *Bz* conditions. Studies based on the simultaneous particle flux data from NOAA POES satellite and Imaging riometer data from Kilpisjarvi (69.05^0 N, 20.79^0 E, geographic coordinates) suggest that the intensity and local time of the particle precipitation and CNA change dramatically during high speed streams (HSS) of the solar wind [Meredith et al., 2011; Kavanagh et al., 2012]. Although our study does not address HSS, we observed that the occurrence frequency of CNA events is independent of the speed of solar wind (Fig. 6a). Nevertheless, there is an indication of increased CNA intensity with increasing solar wind speed. Intensity of southward IMF *Bz* during the substorms clearly increased the level of absorption at Maitri (Fig 6b). It is consistent with the finding of Kavanagh et al. [2004; 2012] that negative IMF *Bz* produces higher CNA across all L-shells and MLT.

The dawn-dusk component of the interplanetary electric field (*Ey*), which depends on solar wind speed and IMF *Bz*, is known to be extremely important for driving geomagnetic activity [e.g., Huang et al., 2005; Chakrabarty et al., 2008]. Maximum intensity of absorption at Maitri (Max (CNA)) almost linearly increased with increasing duskward IEF *Ey* intensity as shown in Fig. 6c.

5. Summary and conclusions

Our analysis of about 1 year magnetometer and riometer data of Maitri station, Antarctica in relation to magnetic substorms and interplanetary conditions suggests that:

1. Onsets of the westward electrojet and cosmic noise absorption at the station were centered around local midnight. Intensity of the electrojet and CNA over Maitri were almost linearly related to the intensity of (northern hemispheric) AL index.
2. At Maitri, westward electrojet and cosmic noise absorption were mainly observed during storm-time substorms possibly due to the location of the station near equatorward boundary of the auroral oval.
3. A clear distinction in the intensity and extent of the absorption region was observed for isolated substorm and storm-time substorm cases. Usually storm-time substorm absorption events were far more intense and covered wide latitude and longitude regions.
4. Magnitudes of the southward IMF *Bz* or duskward IEF *Ey* were linearly related to intensity of CNA at Maitri. Moreover, increasing solar wind speed and IMF *Bz* appear to cause enhancement in the precipitation of harder electrons leading to enhanced CNA.

Acknowledgment:

Authors would like to extend their sincere thanks to the National Centre for Antarctica and Ocean Research (Ministry of Earth Sciences) for providing the necessary infrastructure during the XXX Indian Scientific Expedition to Antarctica, 2009. Authors also acknowledge the OMNIWeb (http://omniweb.gsfc.nasa.gov/form/omni_min.html) for time-shifted interplanetary observations and World Data Centre (WDC), Kyoto (http://wdc.kugi.kyoto-u.ac.jp/aeasy/index.html) for geomagnetic indices.

References:

1. Akasofu, S.-I. Polar and magnetospheric substorms, D. Reidel, Dordrecht, Holland, 1968.
2. Arnoldy, R. L. Auroral particle precipitation and Birkeland Currents. Rev. Geophys. 12(2), 217–231, doi:10.1029/RG012i002p00217, 1974.
3. Alexander Frank-Kamentsky and O. Troshichev, A relationship between the auroral absorption and the magnetic activity in the polar cap. Journal of Atmospheric and Solar-Terrestrial Physics, 77, 40-45, 2011.
4. Arun T., Dhar, A., Emperumal, K., Pathan, B. M. IMF BY dependence of the extent of substorm westward electrojet. J. Earth Syst. Sci. 114, 177–184, 2005.
5. Baker, D. N., Hones, E. W., Belian, R. D., Higbie, P. R., Lepping, R. P., Stauning, P. Multiple-spacecraft and correlated riometer study of magnetospheric substorm phenomena. J. Geophys. Res. 87, 6121-6136, doi:10.1029/JA087iA08p06121, 1982.
6. Behera, J. K., Sinha, A. K., Singh, A. K., Rawat, R., Vichare, G., Dhar, A., Pathan, B. M., Nair, K. U., Selvaraj, C., Elango, P. First results from imaging riometer installed at Indian Antarctic station Maitri. J. Earth Syst. Sci. 123(3), 593-602, 2014.
7. Birch, M. J., Hargreaves, J. K., Bromage, B. J. I. Properties of auroral radio absorption patches observed in the noon sector using imaging riometer and incoherent-scatter radar. J. Atmos. Sol. Terr. Phys. 105-106, 262–272, 2013.
8. Birn, J., Thomsen, M. F., Borovsky, J. E. Reeves, G. D., McComas, D. J., Belian, R. D. Characteristic plasma properties during dispersionless substorm injections at geosynchronous orbit. J. Geophys. Res., 102(A2), 2309–2324, doi:10.1029/96JA02870, 1997.
9. Browne, S., Hargreaves, J. K., and Honary, B.: An imaging riometer for ionospheric studies, Electronics and Communication, 7, 209-217, 1995.
10. Burns, C. J., Howarth, W. G., Hargreaves, J. K. High-resolution incoherent scatter radar measurements during electron precipitation events. J. Atoms. Terres. Phys. 52 (3), 205-218. 1990.
11. Chakrabarty, D., Sekar, R., Sastri, J. H., Ravindran, S. Distinctive effects of interplanetary electric field and substorm on nighttime equatorial F layer: A case study. Geophys. Res. Lett. 35, L19108, doi:10.1029/2008GL035415, 2008.
12. Davis, T., Sugiura, M. Auroral electrojet activity index ae and its universal time variations. J. Geophys. Res. 71, 785–801, 1966.
13. Detrick, D. L., Rosenburg, T. J. A Phased-Array Radio wave Imager for Studies of Cosmic Noise Absorption. Radio Sci. 25, 325–338, 1990.
14. Feldstein, Y. I., Popov, V. A., Cumnock, J. A., Prigancova, A., Blomberg, L.G., Kozyra, J. U., Tsurutani, B. T., Gromova, L. I., Levitin, A. E. Auroral electrojets and boundaries of plasma domains in the magnetosphere during magnetically disturbed intervals. Ann. Geophys. 24, 2243-2276, 2006.
15. Gonzalez, W. D., Tsurutani, B. T. Criteria of interplanetary parameters causing intense magnetic storms (Dst < -100 nT). Planet. Space Sci. 35, 1101–1109, 1987.
16. Hargreaves, J. K. Auroral Absorption of HF Radio Waves in the Ionosphere: A Review of Results from the First Decade of Riometry. Proceedings of the IEEE, 57, 1348–1373, 1969.

17. Hargreaves, J. K. Dynamics of auroral absorption in the midnight sector - The movement of absorption peaks in relation to the substorm onset. Planet. Space Sci. 22, 1427–1441, 1974.

18. Hargreaves, J. K., Browne, S., Ranta, H., Ranta, A., Rosenberg, T. J., Detrick, D. L. A study of substorm-associated nightside spike events in auroral absorption using imaging riometers at South Pole and Kilpisjärvi. J. Atmos. Sol. Terr. Phys., 59 (8), 853–872, 1997.

19. Hanchinal, A.H, Jeeva, K., Ajay Dhar and Girija Rajaram. Response of Geomagnetic Field at Indian Antarctic Station Maitri, to increasing Electromagnetic disturbance in Geospace. Technical Publication (Twelfth Indian Expedition to Antarctica), 10, 47-57,1996.

20. Huang, C.-S., Foster, J. C., Kelley, M. C. Long-duration penetration of the interplanetary electric field to the low-latitude ionosphere during the main phase of magnetic storms. J. Geophys. Res. 110, A11309, doi:10.1029/2005JA011202, 2005.

21. Jussila, J. R. T., Aikio, A. T., Shalimov, S., Marple, S. R. Cosmic radio noise absorption events associated with equatorward drifting arcs during a substorm growth phase. Ann. Geophys. 22, 1675–1686, 2004.

22. Kavanagh, A. J. Energy deposition in the lower auroral ionosphere through energetic particle precipitation. Ph. D. Thesis, Univ. of Lancaster, Lancaster, U. K, 2002(a).

23. Kavanagh, A. J., Honary, F., McCrea, I. W., Donovan, E., Woodfield, E. E., Manninen, J., Anderson, P. C. Substorm related changes in precipitation in the dayside auroral zone – a multi instrument case study, Ann. Geophys. 20, 1321–1334, 2002(b).

24. Kavanagh, A. J., Kosch, M. J., Honary, F., Senior, A., Marple, S. R., Woodfield, E. E., McCrea, I. W., The statistical dependence of auroral absorption on geomagnetic and solar wind parameters. Ann. Geophys. 22, 877-887, 2004.

25. Kavanagh, A. J., Honary, F., Donovan, E. F., Ulich, T., Denton, M. H. Key features of >30 keV electron precipitation during high speed solar wind streams: A superposed epoch analysis. J. Geophys. Res. 117, A00L09, doi:10.1029/2011JA017320, 2012.

26. Kellerman, A. C., Makarevich, R. A. The response of auroral absorption to substorm onset: Superposed epoch and propagation analyses. J. Geophys. Res. 116, A05312, doi:10.1029/2010JA015972, 2011.

27. Kikuchi, T., Yamagishi, H., Lester, M. Drift of auroral absorption due to the magnetospheric convection observed with the scanning narrow beam riometer during SUNDIAL. Ann. Geophys. 8, 431-440, 1990.

28. Korotova, G. I., Sibeck, D. G., Rosenberg, T. J., Russell, C. T., Friis-Christensen, E. High-latitude ionospheric transient events in a global context. J. Geophys. Res. 102(A8), 17499–17508, doi:10.1029/97JA00939, 1997.

29. Kullen, A., Karlsson, T. On the relation between solar wind, pseudobreakups, and substorms. J. Geophys. Res. 109, A12218, doi:10.1029/2004JA010488, 2004.

30. Liou, K., Newell, P. T., Shue, J.-H., Meng, C.-I., Miyashita, Y., Kojima, H., Matsumoto, H. "Compression aurora": Particle precipitation driven by long-duration high solar wind ram pressure. J. Geophys. Res. 112, A11216, doi:10.1029/2007JA012443, 2007.

31. Meredith, N. P., Horne, R. B., Lam, M. M., Denton, M. H., Borovsky, J. E., Green, J. C.. Energetic electron precipitation during high-speed solar wind stream driven storms. J. Geophys. Res. 116, A05223, doi:10.1029/2010JA016293, 2011.

32. Newell, P. T., Meng, C.-I. Mapping the dayside ionosphere to the magnetosphere according to particle precipitation characteristics. Geophys. Res. Lett. 19 (6), 609-612, 1992.
33. Nielsen, E. Dynamics and spatial scale of auroral absorption spikes associated with the substorm expansion phase. J. Geophys. Res. 85, 2092–2098, 1980.
34. Partamies, N., Juusola, L., Tanskanen, E., and Kauristie, K. Statistical properties of substorms during different storm and solar cycle phases. Ann. Geophys. 31, 349-358, doi:10.5194/angeo-31-349-2013, 2013.
35. Ranta, H., Ranta, A., Collis, P. N., Hargreaves, J. K. Development of the auroral absorption substorm: Studies of pre-onset phase and sharp onset using an extensive riometer network. Planet. Space Sci. 29, 1287-1313, 1981.
36. Singh, A. K., Sinha, A. K., Rawat, R., Jayashree, B., Pathan, B. M., Dhar, A. A broad climatology of very high latitude substorms. Adv. Space Res. 50, 1512-1523, doi:10.1016/j.asr.2012.07.034, 2012.
37. Sotirelis, T., Korth, H. Hsieh, S.-Y., Zhang, Y., Morrison, D., Paxton, L. Empirical relationship between electron precipitation and far-ultraviolet auroral emissions from DMSP observations. J. Geophys. Res. Space Physics. 118, 1203–1209, doi:10.1002/jgra.50157, 2013.
38. Spanswick, E., Donovan, E., Friedel, R., Korth, A. Ground based identification of dispersionless electron injections. Geophys. Res. Lett. 34, L03101, doi:10.1029/2006GL028329, 2007.
39. Stauning, P. Investigations of ionospheric radio wave absorption processes using imaging riometer techniques. J. Atmosp. Terr. Phys. 58 (6), 753-764, 1996.
40. Tsurutani, B. T., Gonzalez, W. D. The cause of high-intensity long-duration continuous AE activity (HILDCAAs): Interplanetary Alfvén wave trains. Planetary Space Sci. 35, 405-412, 1987.
41. Vichare, G., Rawat, R., Hinchanal, A., Sinha, A. K., Dhar, A., Pathan, B. M. Seasonal evolution of Sq current system at sub-auroral latitude. Earth Planets Space. 64, 1023-1031, 2012.
42. Weygand, J. M., Zesta, E. Comparison of auroral electrojet indices in the Northern and Southern Hemispheres. J. Geophys. Res. 113, A08202, doi:10.1029/2008JA013055, 2008.
43. Weimer, D. R., King, J. H. Improved calculations of interplanetary magnetic field phase front angles and propagation time delays. J. Geophys. Res. 113, A01105, doi:10.1029/2007JA012452, 2008.
44. Wilson, A., Stoker, P. H. Imaging riometer observations on energetic electron precipitation at SANAE IV, Antarctica. J. Geophys. Res. 107 (A10), 1268, doi:10.1029/2000JA000463, 2002.
45. Wing, S., Gkioulidou, M., Johnson, J. R., Newell, P. T., Wang, C.-P., Auroral particle precipitation characterized by the substorm cycle. J. Geophys. Res. 118, 1022–1039, doi:10.1002/jgra.50160, 2013.